EPJ manuscript No.
(will be inserted by the editor)

On the account of final state correlation in double ionization processes.

I. A. Ivanov[1], A.S.Kheifets[1], and J.Dubau[2]

[1] Research School of Physical Sciences and Engineering, The Australian National University, Canberra ACT 0200, Australia

[2] Universite Paris-Sud, F-91405 Orsay, France

Received: date / Revised version: date

Abstract. We discuss the use of uncorrelated final state wave functions in calculations of double ionization processes. We show that in some physical situations such a simplified treatment can provide meaningful results. In particular, the prevalence of back-to-back emission in two-photon double ionization and even energy sharing between the photoelectrons make it possible to use uncorrelated final state wave functions for total integrated cross-section calculations.

PACS. 32.80.Fb Photoionization of atoms and ions – 42.50.Hz Strong-field excitation of optical transitions in quantum systems; multiphoton processes; dynamic Stark shift – 32.80.Rm Multiphoton ionization and excitation to highly excited states

1 Introduction

Single-photon double ionization (conventional double photoionization or DPI) and two-photon double ionization (TPDI) of atomic or molecular targets are processes in which the system ejects two electrons after absorbing one or two photons, respectively, from the external electromagnetic (EM) field. These processes have considerable appeal to a theorist. On the one hand, they are comparatively simple to allow a completely *ab initio* treatment. On the other hand, they still present serious conceptual and computational challenges. Addressing these challenges have contributed considerably to development and perfection of various theoretical and computational schemes.

The helium atom is the simplest atomic target in which the DPI and TPDI processes can be observed. DPI of He has been studied extensively over the recent years and a broad consensus has been achieved between theory and experiment. On the other hand, TPDI of He is still a

challenging process both for theory and experiment. Even the least detailed total integrated cross-section (TICS) is hotly disputed among various groups. Over the past decade, a large number of theoretical predictions have appeared in the literature [1–15]. These results were obtained by using different theoretical methods such as the many-electron many-photon theory [1], the lowest order perturbation theory [2,15], the R-matrix Floquet approach [5], the method of exterior complex scaling [11], the flux formula [12], and various time-dependent approaches [4,3, 6–10,13,14]. In no way does this list exhaust the literature on the subject as an extended review of the field is beyond the scope of the present paper.

Many of the time-dependent methods mentioned above share the same computational strategy. First, a solution is sought of the equations governing the evolution of the system driven by the external EM field. Second, this solution is projected on the states representing the doubly ionized continuum of the system in the field-free state. It is the projection operation that represents the most difficult part of the problem. Indeed, an accurate description of the atomic or molecular state with two electrons in continuum is a notoriously difficult problem. It may be because of this difficulty that results obtained by different computational methods strongly disagree. A stark example of such a disagreement is the problem of TPDI of helium. In the region of photon energies near 45 eV, disparity of results among various groups may reach a factor of three or even more (see Figure 1 and further discussion in the text below). Correct description of the final doubly ionized state, being sufficiently complicated for an atomic system, becomes even more challenging in theoretical studies of DPI of molecules [16,17].

Various approaches were used to describe the final state of double ionization processes. In works [3,18,16, 14] the final state was represented by a product of two Coulomb waves, thus neglecting the final state correlation completely. In Ref. [4], the correlation in the final state was accounted for by means of the perturbation theory. In the R-matrix Floquet calculation [5] and works [7,8,2], the authors used non-perturbative correlated final state wave functions constructed in various ways. A similar non-perturbative description was used in Ref. [15,10] by means of the convergent close-coupling (CCC) method [19].

Despite of very different treatment of the final state correlation, various calculations of TDPI of helium may give sometimes quite similar results. For example, the total integrated cross-section (TICS) reported in [3,14] agree well with the results published in [5], and with our earlier results [15,10]. The works [3,14] employed an uncorrelated final state, while in Ref. [5,15,10] various representations of the correlated final states were used. Nevertheless, all these methods give the TICS value around one unit of 10^{-52} cm^{4}s at the photon energy $\omega = 45$ eV (see corresponding values in Figure 1). On the other hand, fully correlated and non-correlated results of the J-matrix calculation reported in [7] differ by nearly an order of magnitude (compare J-matrix FC and NC results in Figure 1).

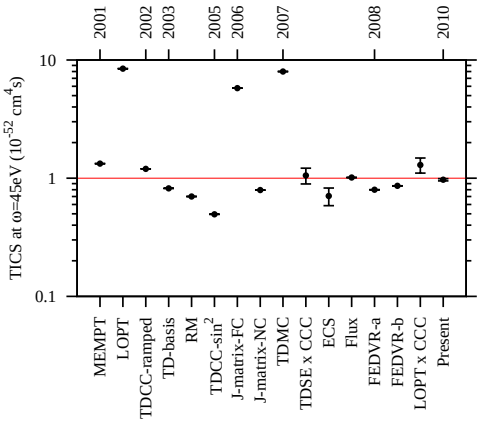

Fig. 1. Total integrated cross section (TICS) of TPDI of He at the photon energy $\omega = 45$ eV. The literature data are marked (from left to right in chronological order) as follows: many-electron many-photon theory (MEMPT) [1], lowest order perturbation theory (LOPT) [2], time-dependent close-coupling (TDCC) with ramped envelope [3], time-dependent (TD)-basis [4], R-matrix [5], TDCC with $\sin^2$ envelope [6], J-matrix with final correlation (FC) and no correlation (NC) [7], time-dependent multi-channel (TDMC) [9], time-dependent Schrödinger equation (TDSE) projected on the convergent close-coupling final state (TDSE×CCC) [10], exterior complex scaling (ECS) [11], flux formula [12], finite element discrete variable representation (FEDVR-a) [13] and (FEDVR-b)[14], LOPT projected on CCC (LOPT×CCC) [15]. The time line of publications is marked on the top horizontal scale of the plot.

An explicit description of the final doubly ionized state can be avoided altogether. For instance, the ionization amplitude can be extracted from the wave function with the help of the so-called Peterkop formalism [20,21]. An approach based on this formalism was applied to DPI of the hydrogen molecule [17] and TPDI of helium [11,22]. Incidentally, in the helium works, the authors obtained TICS results which were rather close to the mentioned above results of the work [3], where an uncorrelated representation of the final state was used. Conceptually similar formalism was used in the work [12], where a flux formula was employed to extract TICS for DPI and TPDI of He without explicit knowledge of the final-state continuum wave function. Again, their TICS results were close to one unit of 10^{-52} cm^{4}s at the photon energy $\omega = 45$ eV (see Figure 1). Yet another method allowing to obtain information about ionization probabilities from the solution of TDSE without knowledge of the wavefunctions of the continuum states was proposed in [23].

As we mentioned above, the use of a fully correlated final state can produce TICS results which agree with calculations neglecting this correlation or accounting for it implicitly by means of the Peterkop formalism. The use of an uncorrelated final state offers a considerable computational advantage. It is desirable, therefore, to understand why and when results obtained by using uncorrelated and correlated final states agree. This fact prompted us to perform a study which we present below. As an object of this study, we choose TPDI process in helium.

2 Theory and results.

We seek a solution of the time-dependent Schrödinger equation (TDSE) for the helium atom in the presence of an external EM field:

$$i\,\partial\Psi/\partial t = \left[\hat{H}_{\rm atom} + \hat{H}_{\rm int}(t)\right]\Psi\ , \qquad (1)$$

where $\hat{H}_{\rm atom}$ is the Hamiltonian of a field-free atom, the operator $\hat{H}_{\rm int}(t)$ describes interaction of the atom and the EM field. We use below both the velocity and length forms of this operator:

$$\hat{H}_{\rm int}(t) = \begin{cases} \boldsymbol{E}(t)\cdot(\boldsymbol{r}_1+\boldsymbol{r}_2)\ , & \text{Length} \\ \boldsymbol{A}(t)\cdot(\hat{\boldsymbol{p}}_1+\hat{\boldsymbol{p}}_2)\ , & \text{Velocity} \end{cases} \quad (2)$$

Here $\boldsymbol{A}(t) = -\int\limits_0^t \boldsymbol{E}(\tau)\,d\tau$. The EM field is $\boldsymbol{E}(t) = f(t)\boldsymbol{E}_0\cos\omega t$, where the envelope function $f(t)$ is chosen in the following way. The amplitude of the AC field remains constant during the time interval $(T, T_1 - T)$, where $T = 2\pi/\omega$ is a period of the AC field, $T_1 = 8T$ is the total duration of the pulse. The field is ramped on and off smoothly over one AC field period. The AC electric field is assumed to be linearly polarized along the z-axis. In the calculations below we shall use E_0=0.1 a.u. a.u. (corresponding to the field intensity of 3.5×10^{14} W/cm^2) for the value of the peak strength of the EM field.

In the velocity gauge, we omitted the quadratic $\boldsymbol{A}^2(t)$ term in the interaction Hamiltonian (2). This term can always be removed through a gauge transformation [24], which amounts to multiplying the wave function by a phase factor. This is unimportant as long as we rely on the dipole approximation which is adopted in the present work.

We discretize the TDSE on a spatial grid with the step $\Delta r = 0.1$ a.u. using a box of the size $R_{\rm max} = 100$ a.u. Temporal grid is equidistant, for each layer t_n the wave function is represented as a superposition:

$$\Psi(\boldsymbol{r}_1,\boldsymbol{r}_2,t_n) = \sum_{l_1,l_2,J} f^J_{l_1l_2}(r_1,r_2,t_n)|l_1(1)l_2(2)\ L\rangle\ , \quad (3)$$

where notation $|l_1(1)l_2(2)\ L\rangle$ is used for bipolar harmonics [25], the functions $f^J_{l_1l_2}(r_1,r_2,t_n)$ are defined in the points of the grid, summation in Eq. (3) is restricted to $l_1, l_2 = 0-3$, $J = 0-2$.

For each layer t_n we propagate the wave function (3) in the coordinate grid from the origin using the three-point finite difference formula for the second and first (in velocity gauge) spatial derivatives. Transparent boundary conditions [26] are imposed on the functions $f^J_{l_1l_2}$ on the boundary of the box. The time propagation of Eq. (3) is performed by two different methods. We employ the two-step Euler method and, as a double check, the method based on the Arnoldi propagator [27–29]. Both methods are explicit, which makes them convenient in handling large scale problems. For the propagation based on the only conditionally stable two-step Euler method, we have to choose a sufficiently small time-step taken presently at 6×10^{-4} a.u. The Arnoldi method represents the wave function at time $t_n + \Delta t$ as a superposition of the vectors from the Krylov space formed by the vectors $\Psi(t_n), \hat{H}\Psi(t_n), \ldots \hat{H}^m\Psi(t_n)$. We used $m = 4$. This procedure is unconditionally stable allowing to use a larger time-step.

Initial state of the helium atom was found by using a relaxation procedure, which gave us an acceptable value of -2.869 a.u. for the He ground state energy. After the end of the pulse at $T_1 = 8T$, we let the system evolve freely retaining only the atomic Hamiltonian in the TDSE. At times $t = 8T, 9T, 10T, 11T$ we compute the expectation values $\langle\Psi(T_1)|\hat{P}|\Psi(T_1)\rangle$ with the projection operator $\hat{P}$

being built using the properly symmetrized product of uncorrelated Coulomb waves for the attractive charge $Z = 2$.

For the problem of TPDI of helium, the operator $\hat{P}$ includes states with total angular momenta $J = 0, 2$ (S- and D- waves). For the S-wave, we have to take into account the fact that the Coulomb waves are not orthogonal to the ground state $\hat{P}\Psi_{\rm ground} \neq 0$. We follow the recipe outlined in the work [3] and use the wave function $\tilde{\Psi} = \Psi - \langle\Psi_{\rm ground}|\Psi\rangle\Psi_{\rm ground}$ which is orthogonal to the ground state.

The total integrated cross-section (TICS) of double ionization process can be calculated as:

$$\sigma = CW^{-1}\langle\tilde{\Psi}(t)|\hat{P}|\tilde{\Psi}(t)\rangle \ . \qquad (4)$$

For the TPDI process, $W = \int_0^{T_1} \boldsymbol{E}^4(t)\ dt$, the constant $C = 12\pi^2 a_0^4 \tau\omega^2 c^{-2}$, where $c \approx 137$ is the speed of light in atomic units, Bohr radius $a_0 = 0.529 \times 10^{-8}$ cm and atomic unit of time $\tau = 2.418 \times 10^{-17}$ s.

In Table 1 we present the results for TICS of TPDI for helium in the length and velocity gauges, which we obtained for the photon energy of 45 eV. The EM pulse duration was eight optical cycles $T_1 = 8T$, for $t > T_1$ the system was allowed to propagate freely. A rather satisfying conclusion which one can draw from inspection of Table 1 is good agreement between the length and velocity gauges. This means that the TDSE is solved accurately and also that the ranges of summations over the angular momenta values in Eq. (3) are chosen properly. The wave functions in the length and velocity gauges differ by a factor $\exp[i\boldsymbol{A}\cdot\boldsymbol{r}]$. This implies that a given number of partial waves may represent the wave function adequately in one gauge but not so well in the other. In many cases use of the velocity gauge is more economical as far as convergence of the partial wave expansions is concerned [30,31].

Table 1. TICS of TPDI for helium, in units of 10^{-52} cm^{4}s, computed in the length and velocity gauges for different field-free propagation times after the end of the EM pulse. The field parameters are as follows: the peak strength $E_0 = 0.1$ a.u., the photon energy $\omega = 45$ eV.

Gauge	Time			
	$8T$	$9T$	$10T$	$11T$
	S-wave			
L	0.295	0.301	0.307	0.308
V	0.298	0.304	0.310	0.310
	D-wave			
L	0.703	0.709	0.709	0.710
V	0.694	0.700	0.701	0.701

These observations allow us to conclude that the wave function Ψ at the end of the pulse, or several periods after the end of the pulse, is known with good accuracy. This fact by itself, however, does not guarantee that the projection on uncorrelated Coulomb waves in Eq. (4) should produce physically meaningful results.

The sum of the partial wave contributions from Table 1 gives the TICS values of approximately 1.0×10^{-52} cm^{4}s at the photon energy $\omega = 45$ eV . Not surprisingly, this result agrees well with the corresponding value of 1.2×10^{-52} cm^{4}s reported in the work [3], where the same set of uncorrelated final states and a similar ramped EM pulse were used. We checked that our TICS results do

not depend in a sensitive way on the particular shape of the EM pulse. With the envelope function $f(t) = \sin^2 \pi t/T_1$ and the same set of field parameters, we obtained the TICS value of 1.05×10^{-52} cm^{4}s.

More surprising is the fact that the present TICS values are quite close to our earlier TDSE result of $(1.05 \pm 0.15) \times 10^{-52}$ cm^{4}s [10] and the LOPT result of $1.3 \pm 0.2 \times 10^{-52}$ cm^{4}s [15]. Both calculations employed the correlated CCC final state wave functions. As we mentioned above, a few other approaches [12,11,22] relying on different methods to represent correlated final state gave results close to this value. On the other hand, authors of the work [7,8] found, that use of the fully correlated final state in the framework of their approach gave a considerably larger value for TICS than the value obtained by projecting their solution of TDSE on the uncorrelated Coulomb waves. This latter value (marked as J-matrix NC results in Figure 1)) is sufficiently close to the value of $(1.0 \times 10^{-52}$ cm^4. Results of the three calculations, where solution of TDSE has been projected on uncorrelated final states (work [3], J-matrix NC calculation of the work [7] and the present work) agree reasonably well. This probably means that different methods employed for the solution of TDSE in these works produced similar results for the wavefunction after the end of the pulse.

To obtain the correlated results (marked as NC in Figure 1) the following procedure has been used in [7]. Using the J-matrix technique authors solve first a simpler problem of constructing the states of the single continuum, which allows to extract the single-continuum component from the total wavefunction. Extracting further the bound states contributions, authors obtained the double-continuum component of the wavefunction, which was used to evaluate TICS of TPDI. This procedure thus avoid completely the complicated question of the description of the states of double continuum. At the same time, this is an indirect way to compute TICS. The fact that double-continuum component of the wavefunction is considerably smaller than the bound states and single-continuum contributions may impose rather stringent requirements on the accuracy of the calculation.

As we have seen above, at least in some cases, results obtained using the correlated and uncorrelated final states agree quite well.

A look at the time-dependence of the partial wave contributions in Table 1 may provide some clues as to why and how it may happen. Let us switch to the Heisenberg representation in Eq. (4) for the times $t > T_1$ corresponding to free evolution of the atom after the end of the EM pulse. The projection operator in this representation will take the form $\hat{P}(t) = e^{i\hat{H}_{\rm atom}(t-T_1)}\hat{P}e^{-i\hat{H}_{\rm atom}(t-T_1)}$. We shall use the notation $\hat{P}_{\rm true}$ for the projection operator on the manifold of doubly ionized states of the helium atom, built with the help of the exact correlated wave functions. This operator is time-independent. In no sense relying on the concept of the operator norm, can $\hat{P}(t)$ converge to $\hat{P}_{\rm true}$ for $t \to \infty$. We may, however, expect that the matrix elements of $\hat{P}(t)$ may converge to the matrix elements of $\hat{P}_{\rm true}$ for some special choices of the wave function $\tilde{\Psi}(T_1)$ in Eq. (4).

The criterion often used for justifying the validity of the projection on non-correlated states in calculations of double ionization phenomena is the dominance of the kinetic energy over its potential counterpart [16]. This criterion, in fact, may be too restrictive. A classical estimate shows that, for the photon energy of 45 eV, the two photoelectrons with equal energy sharing (5.5 eV each), after having traveled away from the nucleus for the time $T_1 = 8T$, will still have comparable kinetic and potential energies. Thus, the observed near constancy of the probabilities in Table 1 cannot be explained by the energy criterion alone.

More detailed view of the two-electron dynamics is provided by the asymptotic form of the final state wave function. Various asymptotic forms corresponding to different regions of the configuration space are known [32–34]. At the photon energy $\omega = 45$ eV, the single differential (with respect to energy) cross-section (SDCS) of TPDI is almost flat [3]. This means that an extremely unequal energy sharing between the photoelectrons is not very likely. The TPDI process also favors a strong back-to-back emission [35,8]. This is a result of the electron correlation [8] and the fact, that for TPDI the inter-electron repulsion is not dampen by the dipole selection rule.

Therefore, a typical spatial configuration of the two-electron escape is characterized by large quantities r_1, r_2 and r_{12}. This is the so-called Redmond asymptotic region [32,33] in which the two-electron continuum wave function takes the form $\exp\left(i\boldsymbol{k}_1\cdot\boldsymbol{r}_1 + i\boldsymbol{k}_2\cdot\boldsymbol{r}_2 + i\gamma\right)$ with the phase factor

$$\gamma = \frac{2}{k_1}\ln\left(\boldsymbol{k}_1\cdot\boldsymbol{r}_1 + k_1 r_1\right) + \frac{2}{k_2}\ln\left(\boldsymbol{k}_2\cdot\boldsymbol{r}_2 + k_2 r_2\right) - \frac{1}{k_{12}}\ln\left(\boldsymbol{k}_{12}\cdot\boldsymbol{r}_{12} + k_{12} r_{12}\right) . \quad (5)$$

Here $\boldsymbol{k}_{12} = \boldsymbol{k}_1 - \boldsymbol{k}_2$ and $\boldsymbol{r}_{12} = \boldsymbol{r}_1 - \boldsymbol{r}_2$. This form is a product of two Coulomb waves with $Z = 2$ modulated by a factor depending on the vectors of the relative position and momentum. For the case of comparable values of k_1, k_2 and back-to-back emission, when k_{12} is greater than k_1 and k_2, this modulation is relatively shallow and can be considered as a relatively weak modulation of the nucleus charge. Thus, in the situation when electrons are ejected predominantly back-to-back with nearly equal velocities, the projector built from the product of the Coulomb waves may approximate the true projector on the doubly ionized states in Eq. (4) reliably.

We can present another evidence that it is the Redmond asymptotic region (with r_1, r_2 and r_{12} being large) that is the most important for rendering essential features of the TPDI process. To do so, we built the projection operator in Eq. (4) from the symmetrized product of two Coulomb waves with $Z_1 = 1$ and $Z_2 = 2$, which corresponds to the physical picture of screening. Results of such a calculation in the length and velocity gauges are shown in Figure 2, together with the results obtained using the data from Table 1. One can see that the TICS values computed using such a projection operator are considerably larger. More importantly, they vary considerably stronger with time. This fact suggests that computations of TICS

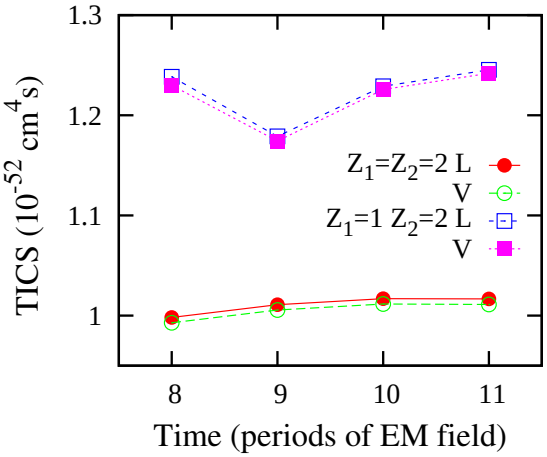

Fig. 2. (Color online). Total integrated cross section of TPDI of helium computed for different periods of field-free evolution after the end of the EM pulse. Calculations with equal asymptotic charges $Z = 2$ are shown with filled (L-gauge) and open (V-gauge) circles. Corresponding results with unequal charges $Z_1 = 1$ and $Z_2 = 2$ are displayed with filled (L-gauge) and open (V-gauge) squares. The field parameters are the same as in Table 1

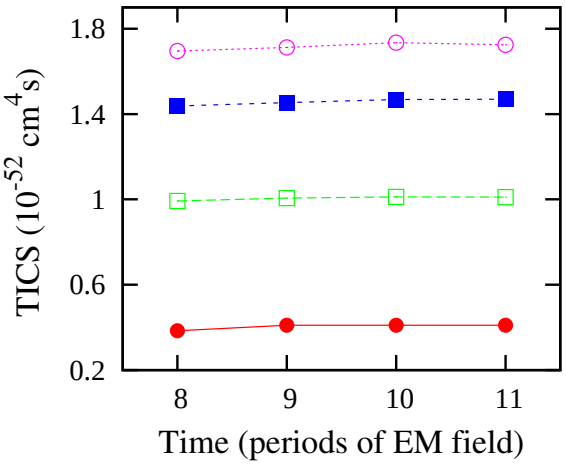

Fig. 3. (Color online). Total integrated cross section of TPDI of helium computed for different periods of field-free evolution after the end of the pulse for photon energies of 42 eV (filled circles), 45 eV (open squares), 48 eV (filled squares) and 50 eV (open circles). Calculations are in the velocity gauge.

using such a projection operator cannot produce accurate results.

The premises on which we based our justification of the use of uncorrelated Coulomb functions for calculation of TICS of TPDI were back-to-back emission of the photoelectrons and a reasonably flat SDCS. For the photon energies approaching the sequential ionization (SI) threshold (54.4 eV in He), these premises will not hold so well as for the photon energy of 45 eV which we considered above. Indeed, it was shown in Ref. [22] that, upon approaching the SI threshold, the SDCS starts growing rapidly at the edges of the excess energy interval favoring an unequal energy sharing. This " virtual SI" effect can be considered as a manifestation of the transition to the SI regime in which the two photoelectrons have well-defined and different energies. We can expect also that back-to-back emission is not so strongly dominant for photon energies approaching the SI threshold. In fact, for the truly SI regime, the angular distribution of the escaped electrons can be approximately described as a product of two dipole distributions [11], in which no trace of the dominance of the back-to-back emission is present. Thus, we can expect that, for the photon energies approaching the SI threshold, the use of uncorrelated Coulomb functions for TICS calculation will give less reliable results.

As an illustration of this statement, we present in Figure 3 the TICS of TPDI computed for the photon energies of 42, 48 and 50 eV. As above, the peak strength of the EM field was 0.1 a.u., the total duration of the pulse was 8 cycles. We present only velocity gauge results. As for the

case of the photon energy of 45 eV, two gauges produce nearly identical results. One can see that, if the atom is left to evolve freely, the TICS results for 48 and 50 eV vary considerably more with time than it was the case for the photon energy of 45 eV, in agreement with the reasoning we presented above.

3 Conclusion.

In this paper, we studied the role of the final state correlation in the double ionization processes. In particular, we investigated the conditions and limits of use of uncorrelated final state wave functions. If such conditions and limits could be established, it would simplify considerably the calculations. We illustrated our findings by various calculations of the total integrated cross-sections of TPDI of helium at several selected photon energy points. Our computational technique is based on the solution of the time-dependent Schrödinger equation and subsequent projection of the solution on a properly symmetrized product of the Coulomb waves. We demonstrated that in some cases the projection operator $\hat{P}$ built from these Coulomb waves may share an important property with the true projection operator on the exact doubly ionized states. The TICS results obtained with the aid of such a projection operator depend only very weakly on time if system is allowed to evolve freely after the end of the EM pulse.

For the presently employed field parameters, such a behavior of TICS cannot be explained in terms of the ratio of the potential and kinetic energies of photoelectrons. Neither can it be based on the drop-off of the Coulomb-induced logarithmic phase distortion considered in Ref. [23] as the photoelectrons do not travel sufficiently large distances. To explain this phenomenon, we rely on the known asymptotic expression of the wave function describing the two photoelectrons escaping back-to-back with comparable velocities. This is the dominant escape configuration of TPDI for the photon energies not too close to the SI threshold. In such a situation, the use of an uncorrelated product of the Coulomb waves to represent the final state can give accurate TICS results. This by no means implies, that electron correlation is not important in this case. On the contrary, for TPDI in helium, for example, electron correlation plays very important role [8]. Important, however, is that in this case effect of the electron correlation leads to the dominance of electron configurations with nearly equal energies and opposite momenta, which are the conditions on which we based the discussion presented above.

If either of these conditions is not fulfilled, the use of uncorrelated Coulomb waves may give less accurate results, as we saw above for the TPDI process with photon energy approaching the SI threshold. Use of the uncorrelated final state wavefunctions can also be expected to give less accurate results for the calculations of the cross-section of the single-photon double ionization (DPI) of helium. At the photon energies sufficiently close to the DPI threshold, the SDCS of this process is a flat curve as prescribed by the Wannier theory. It is the assumption of the dominance of the back-to-back emission that is not

valid in this case, this configuration being suppressed by the dipole selection rules.

4 Acknowledgements

The authors acknowledge support of the Australian Research Council in the form of the Discovery grant DP0985136. Computational work was carried out at the Australian National Computational Infrastructure (NCI) Facility.

References

1. T. Mercouris, C. Haritos, C.A. Nicolaides, J. Phys. B **34**, 3789 (2001)
2. L.A.A. Nikolopoulos, P. Lambropoulos, J. Phys. B **34**, 545 (2001)
3. J. Colgan, M.S. Pindzola, Phys. Rev. Lett. **88**, 173002 (2002)
4. B. Piraux, J. Bauer, S. Laulan, H. Bachau, Eur. Phys. J. D **26**, 7 (2003), http://dx.doi.org/10.1140/epjd/e2003-00063-3
5. L. Feng, H.W. van der Hart, J. Phys. B **36**(1), L1 (2003)
6. S.X. Hu, J. Colgan, L.A. Collins, J. Phys. B **38**, L35 (2005)
7. E. Foumouo, G.L. Kamta, G. Edah, B. Piraux, Phys. Rev. A **74**, 063409 (2006)
8. E. Foumouo, P. Antoine, B. Piraux, L. Malegat, H. Bachau, R. Shakeshaft, J. Phys. B **41**, 051001 (2008)
9. L.A.A. Nikolopoulos, P. Lambropoulos, J. Phys. B **40**(6), 1347 (2007)
10. I.A. Ivanov, A.S. Kheifets, Phys. Rev. A **75**, 033411 (2007)
11. D.A. Horner, F. Morales, T.N. Rescigno, F. Martin, C.W. McCurdy, Phys. Rev. A **76**, 030701(R) (2007)
12. R. Shakeshaft, Phys. Rev. A **76**(6), 063405 (2007)
13. J. Feist, S. Nagele, R. Pazourek, E. Persson, B.I. Schneider, L.A. Collins, J. Burgdörfer, Phys. Rev. A **77**(4), 043420 (2008)
14. X. Guan, K. Bartschat, B.I. Schneider, Phys. Rev. A **77**(4), 043421 (2008)
15. I.A. Ivanov, A.S. Kheifets, J. Phys. B **41**, 095002 (2008)
16. J. Colgan, M.S. Pindzola, F. Robicheaux, J. Phys. B **37**, L377 (2004)
17. W. Vanroose, D.A. Horner, F. Martín, T.N. Rescigno, C.W. McCurdy, Phys. Rev. A **74**(5), 052702 (2006)
18. J. Colgan, M.S. Pindzola, Phys. Rev. A **65**, 032729 (2002)
19. I. Bray, Phys. Rev. A **49**(2), 1066 (1994)
20. R.K. Peterkop, *Theory of Ionization of Atoms by Electron Impact* (Colorado Associated University Press, Boulder, CO, 1977)
21. M.R.H. Rudge, Rev. Mod. Phys. **40**, 564 (1968)
22. D.A. Horner, C.W. McCurdy, T.N. Rescigno, Phys. Rev. A **78**, 043416 (2008)
23. L.B. Madsen, L.A.A. Nikolopoulos, T.K. Kjeldsen, J. Fernández, Phys. Rev. A **76**(6), 063407 (2007)
24. R. Shakeshaft, X. Tang, Phys. Rev. A **36**, 3193 (1987)
25. D.A. Varshalovich, A.N. Moskalev, V.K. Khersonskii, *Quantum theory of angular momentum* (World Scientific, Singapore, 1988)
26. G.R. Hadley, Optics Letters **16**, 624 (1991)
27. T.J. Park, J.C. Light, J. Chem. Phys. **85**, 5870 (1986)
28. D. Dundas, Phys. Rev. A **65**, 023408 (2002)
29. R. Nepstad, H.W. van der Hart, J.F. McCann, J. Phys. B **42**, 145603 (2009)
30. E. Cormier, P. Lambropoulos, Journal of Physics B: Atomic, Molecular and Optical Physics **29**(9), 1667 (1996)

31. M. Nurhuda, F.H.M. Faisal, Phys. Rev. A **60**(4), 3125 (1999)
32. R. Peterkop, J. Phys. B **4**, 513 (1971)
33. R. Peterkop, J. Phys. B **15**, L751 (1982)
34. A. Engelns, H. Klar, A.W. Malcherek, J. Phys. B **30**(22) (1997)
35. A.S. Kheifets, I.A. Ivanov, J. Phys. B **39**(7), 1731 (2006), http://stacks.iop.org/0953-4075/39/1731